

Vincent T. Wood¹ and Luther W. White²

¹NOAA/OAR/National Severe Storms Laboratory, Norman, OK

²Department of Mathematics, University of Oklahoma, Norman, OK

1. INTRODUCTION

The wind field around an intense atmospheric vortex such as a dust devil, tornado and mesocyclone can be accurately depicted using a parametric wind-profile model if the driving parameters are accurately determined. Wood and White (2011, henceforth WW) developed a new parametric model to depict a realistic-looking tangential-wind profile that closely resembles that of any vortex. The profile employs five key parameters: maximum tangential wind, radius of maximum tangential wind, and three power-law exponents that shape different parts of the velocity profile, including a new one that controls the broadly- or sharply-peaked profile in the annular zone of tangential velocity maximum.

The objective of this paper is to test and verify the effectiveness and versatility of the Wood-White parametric wind-profile model by using numerical and analytical tangential wind measurements. The unsteady Burgers (1948)-Rott (1958) vortex model and the tornado numerical tangential-wind outputs of Trapp (2000) represent evolving simulated vortices. The analytical and numerical tangential speeds in the form of radial profiles radiating from the center of the vortex provide useful data and verify the WW parametric model.

2. A PARAMETRIC MODEL FOR TANGENTIAL WIND PROFILE

The new parametric vortex wind-profile model was formulated by Wood and White (2011). The model is given as

$$V(r;\mathbf{m}) = V_x \frac{\rho^k}{[1 + kn^{-1}(\rho^{n/\lambda} - 1)]^\lambda}, \quad 0 < k < n, \quad (1)$$

where V is a tangential velocity that varies with radial distance (r) from a vortex center; $\mathbf{m} = [V_x, R_x, k, n, \lambda]^T$ represents a model vector of the five parameters; R_x is the radius at which a tangential velocity peak value (V_x) occurs; $\rho = r/R_x$ is the dimensionless radial distance from the vortex center; k , n and λ are the power-law parameters that control different parts of the velocity profile, as will be described in the subsequent subsection.

Corresponding author address: Vincent T. Wood, National Severe Storms Laboratory, 120 David L. Boren Blvd. Norman, OK 73072. E-mail: Vincent.Wood@noaa.gov

2.1 The Physical Behaviors of the Tangential Velocity Profiles

The plots in Fig. 1 were prepared in order to help understand the roles of varying k , n and λ values on the behaviors of the radial profile families of tangential velocity at a given height. To facilitate comparison with the profiles, normalized composites are constructed that beneficially preserve the underlying tangential wind structure. Each individual profile is expressed in the convenient dimensionless form utilizing the typical scales, V_x and R_x . The radial profile families of normalized tangential velocity as functions of ρ , k , n and λ are represented by the solid curves with and without being joined by circles and x's (Fig. 1). In each panel of the figure, three varying values of n are presented for a selected value of k . As one progresses from the top panels through middle to the bottom panels, k and n remain unchanged with decreasing λ .

The power-law exponent k in ρ^k of (1) primarily controls the inner tangential velocity profile near the vortex center ($\rho = 0$). When $k < 1$ ($k > 1$), the radial profile has negative (positive) curvature. In other words, the curve turns to the right (left) with increasing ρ . As one progresses from the left panels through middle to the right panels of Fig. 1, the curvature of the tangential velocity profile near $\rho = 0$ progressively changes its direction from negative through zero to positive.

When $k = 1$, the V-shaped profile of tangential velocity near $\rho = 0$ produces zero curvature with increasing ρ . This means that the tangential velocity increases linearly, indicating solid-body rotation of fluid in a vortex core with constant angular velocity (see second column of Fig. 1, for example).

The second power-law exponent n in (1) mainly governs the decay profile beyond R_x . The higher (lower) the n value the more rapidly (slowly) the tangential velocity decreases with ρ . It is important to mention that the velocity profile exists only for $0 < k < n$. When $k = n$, the profile is perfectly flat where the vortex cannot exist.

The last power-law exponent, represented by λ in (1), basically controls the "peakness" of the wind profile, meaning that the region of the highest tangential wind can be made broader or narrower. As λ changes from 1.0 to approximately zero, a rounded peaked profile of

tangential velocity transitions to a sharply-peaked profile. As one progresses from the top panels through middle to the bottom panels of Fig. 1, a more rounded maximum tangential wind becomes increasingly localized with decreasing λ around the radius at which the maximum occurs. As $\lambda \rightarrow 0$, three radial profiles for very different n values merge together in each panel to form one superimposed radial profile at $\rho < 1$.

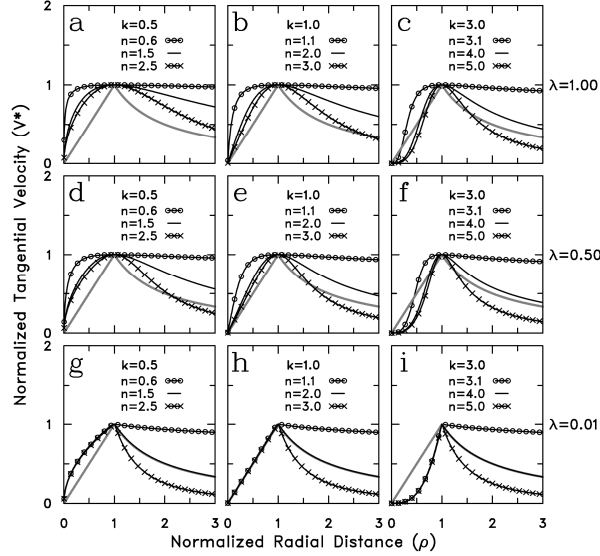


Fig. 1. Radial profile families of normalized tangential velocity (V^*) for selected values of k , n and λ in each panel. Three profile families in each panel are indicated by three different values of n . Gray curves represent the normalized Rankine tangential velocity (V_{RV}^*) for comparison. Normalized radial distance is represented by $\rho = r/R_x$. (After Wood and White 2011).

The model parameters (k, n, λ) do not change the magnitude at $V^* = 1$ and $\rho = 1$. This effect is shown in Fig. 1.

Further insight into the relevant vortex dynamics is obtained by comparing the tangential wind profile of the WW vortex to that of the idealized Rankine (1882) vortex (RV). Consider a normalized Rankine velocity profile, given by

$$V_{RV}^* \equiv \frac{V_{RV}}{V_x} = \rho^\gamma, \quad \begin{cases} \gamma = 1 & \rho < 1 \\ \gamma = 0 & \rho = 1, \\ \gamma = -1 & \rho > 1 \end{cases} \quad (2)$$

where $\rho = r/R_x$ has been defined previously, and γ is the power-law exponent that governs the profiles inside, at and outside $\rho = 1$ (gray curves in Fig. 1). After normalizing the tangential velocity ($V^* = V/V_x$) and setting $k=1$ and $n=2$ in (1), the WW vortex is

transformed to the RV in the following procedure.

Taking the limit of the result as $\lambda \rightarrow 0$, $V^* \rightarrow V_{RV}^* = \rho$

for $\rho \leq 1$. This means that V^* approaches the inner core of solid-body rotation of the RV as one progresses from the top middle column to the bottom middle column (as indicated by black, solid curves in Fig. 1b through Fig. 1e to Fig. 1h). Furthermore, as $\lambda \rightarrow 0$, $V^* \rightarrow V_{RV}^* = \rho^{-1}$ for $\rho > 1$, indicative of the fact that V^* decreases and tends asymptotically to the value given by potential flow in which $V^* \propto \rho^{-1}$. Hence, the WW vortex exactly coincides with the RV when $\lambda \rightarrow 0$. The Rankine vortex may be viewed as a limiting case for the Wood-White vortex as $\lambda \rightarrow 0$.

3. PARAMETRIC VS. NUMERICAL MODELS

A key question that needs to be addressed here is: what is the rationale for developing the parametric tangential-wind profile model in this study? We gain insight into this question by discussing the vast differences between the parametric and dynamical numerical vortex models. As expected, the numerical model makes full use of the Navier-Stokes equations of motion, the continuity of motion and the known physical laws that altogether govern simulated vortices that evolve with time. In order to provide reasonable numerical results for vortex simulations, the numerical model requires a high-resolution grid with properly defined boundary conditions. This process is computationally expensive in terms of execution time and computer memory. On the other hand, the parametric model calculates an *approximation* of the numerical vortex wind fields (such as radial profiles of tangential wind) only if the driving parameters are properly determined. The parametric model offers an attractive alternative because the model improves execution-time costs and preserves most of the validity of the numerical results. While it is true that the high-resolution numerical model remains many investigators' preference over the parametric model, the parametric model still provides an economical and equally good alternative for estimating vortex wind fields (or profiles) for different applications.

Numerous investigators often resort to using different parametric wind models for different applications. In the tropical meteorology community, they used their parametric models to approximate the one- or two-dimensional wind structure within a tropical cyclone in practical applications (e.g., Phadke et. al 2003; MacAfee and Pearson 2006; Jakobsen and Madsen 2004; Holland 1980, 2010; Willoughby and Rain 2004; Willoughby et. al 2006). In the tornado research and engineering communities, Holland (2006) used a simple Rankine model and a modified tree model to simulate tornado damage in forests. Wurman et. al (2007) simulated tornadic winds based on DOW (Doppler on Wheels) radar data to depict wind-induced loss to property.

Can the WW parametric wind-profile model reproduce the tangential wind fields that a high-resolution numerical vortex model generates? This question will be answered in the next section.

4. TESTING AND VERIFICATION

We desire to demonstrate the effectiveness and versatility of the WW model by testing and verifying the model. One theoretical vortex solution of the time-dependent Burgers (1948)-Rott (1958) (henceforth BR) model and one high-resolution numerical vortex model of Trapp (2000) were selected to represent evolving simulated vortices. Interested readers are referred to Trapp (2000) for a more detailed discussion of his numerical model and results. The analytical and numerical tangential speeds in the form of radial profiles radiating from the center of the vortex provide useful data and verify the WW model.

We use the Levenberg (1944)-Marquardt (1963) (LM) optimization method, a standard technique used to solve unconstrained nonlinear least squares problems for curve-fitting applications. The LM method is actually a combination of two minimization methods – the gradient descent method and the Gauss-Newton method. The LM method behaves more like a gradient-descent method when the parameters are far from their optimal value. When the parameters are close to their optimal value, the LM method behaves more like the Gauss-Newton method. The method for implementing the LM algorithm is described in Press et al. (1992).

The LM algorithm is used to fit the WW parameters ($\mathbf{m} = [V_x, R_x, k, n, \lambda]^T$) to the radial profiles of observed (or numerical) tangential velocity output involving minimizing a cost function

$$J(\mathbf{m}) = \sum_{i=1}^{N_{obs}} [V^\ell(r_i; \mathbf{m}) - V_{obs}^\ell(r_i)]^2. \quad (3)$$

Here, V_{obs}^ℓ is the observed (or numerical) tangential velocity data at a given ℓ^{th} height level, r_i is the radial distance from the vortex center, and N_{obs} is the maximum number of gridded tangential velocity output per radial profile at that level. The function accounting for the discrepancy between the model and numerical tangential velocity data is evaluated at each radial profile. At the lowest height level ($\ell=1$) of nonzero numerical (or analytical) tangential velocity data, the guessed values of V_x and R_x are easily determined by scanning one radial profile for the strongest reported tangential velocity and its radial position. The guessed values of power-law exponents (k) and (n), respectively, are determined by reasonably examining the shape profile inside and outside R_x before making initial guess of λ . Fig. 1 may be used as a guideline for estimating the model parameters (k , n , and λ). After having the model parameters (k , n , and λ)

calculated and having available V_x and R_x as inputs to $J(\mathbf{m})$, (3) is minimized by differentiating $J(\mathbf{m})$ with respect to \mathbf{m} , and so the rapidly-converging LM algorithm

$$\frac{\partial J(\mathbf{m})}{\partial \mathbf{m}} = 0. \quad (4)$$

If the iterative process fails to converge, fitting is abandoned. When convergence is achieved, fitting is completed so that the last updated \mathbf{m} values are finalized. Consequently, (1) is computed and stored in a one-dimensional array of fitted tangential velocity to be plotted as a function of radial distance and height. The procedure for minimizing (3) at the next height level ($\ell+1$) is repeated after the updated \mathbf{m} values at the previous (ℓ) height level are assigned to the initial guesses (\mathbf{m}) at that ($\ell+1$) level. The procedure is continued progressively to ($\ell+1$) levels until it is terminated at the top domain of the numerical model.

We calculated the root-mean-square error ($RMSE$) and correlation coefficient (CC), respectively, given by,

$$RMSE = \sqrt{\frac{1}{N_{obs}} \sum (V_{obs} - V_{fit})^2}, \quad (5)$$

and

$$CC = \frac{\sum (V_{obs} - \bar{V}_{obs})(V_{fit} - \bar{V}_{fit})}{\sqrt{\sum (V_{obs} - \bar{V}_{obs})^2 \sum (V_{fit} - \bar{V}_{fit})^2}}, \quad (6)$$

where the sums extend over the N_{obs} analysis grid points for which both observed (obs) and fitted (fit) tangential velocity variables are available, and the overbar represents the sample means of each variable. The two indices in (5) and (6) will be applied to evaluate the accuracy of the fitted and observed tangential-wind profiles.

4.1 The Unsteady Burgers-Rott Vortex Model

Rott (1958) found and Trapp and Davies-Jones (1997) and Davies-Jones and Wood (2006) used an exact unsteady vortex solution of the Navier-Stokes equations of motion and the incompressible continuity equation. The flow parameters used to produce evolution of radial profiles of tangential wind of the time-dependent BR vortex (Fig. 2) were described in Davies-Jones and Wood (2006) for the purpose of testing and verifying the parametric tangential-wind profiles of the WW model.

In steady convergent flow, the unsteady BR vortex amplified but approached a steady state asymptotically as a balance was approached between the inward advection and outward diffusion of angular momentum (Fig. 2). Comparisons of radial profiles of tangential velocity between the BR and WW models are presented in Tables 1 and 2. The fitted wind parameters of V_x and R_x are found to produce and agree with realistic

values of the analytical wind parameters [$V_x(t)$ and $R_c(t)$]. It is interesting to note that approximate potential flow outside the annulus of maximum tangential velocity (indicated by $k-n$ in Table 2) compares favorably with potential flow in the BR model.

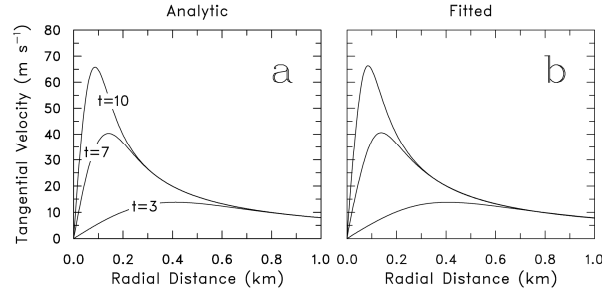


Fig. 2. Evolution of radial profiles of (a) theoretical tangential velocity in the unsteady Burgers-Rott vortex and (b) fitted tangential velocity in the WW parametric vortex at $t = 3, 7$ and 10 min.

TABLE 1. The calculated flow parameters [$V_x(t)$, $R_c(t)$] of the unsteady BR vortex model at $t = 3, 7$ and 10 min for the purpose of comparing to the fitted model parameters of the WW model (see Table 2). Note that $V_x(t)$ represents the unsteady tangential velocity peak; $R_c(t)$ represents the core radius at which $V_x(t)$ occurs. These flow parameters are described in Davies-Jones and Wood (2006)

Model Parameter	$t = 3$	$t = 7$	$t = 10$
$V_x(t)$ ($m s^{-1}$)	14	40	66
$R_c(t)$ (m)	412	141	87

TABLE 2. Fitted model parameters of (V_x , R_x , k , n , λ) used to calculate the radial profiles of the fitted tangential velocity of the WW model are given for comparing to the radial profiles of the unsteady BR tangential velocity (see Table 1) at $t = 3, 7$ and 10 min. Root-mean-square errors (RMSE) and correlation coefficients (CC) are indicated.

Model Parameter	$t = 3$	$t = 7$	$t = 10$
V_x ($m s^{-1}$)	14	41	66
R_x (m)	407	138	86
k	0.901	0.884	0.873
n	2.060	1.932	1.902
λ	0.651	0.547	0.517
$k - n$	-1.159	-1.048	-1.029
RMSE ($m s^{-1}$)	0.058	0.182	0.261
CC	1.000	1.000	1.000

Overall, the comparisons suggest that the WW model does a good job of reproducing tangential wind distribution that well fit to the unsteady BR tangential wind profile. In fact, the parametric model does approximate analytical data as closely as possible.

4.2 Numerical model of Trapp (2000)

Figure 3 compares the vertical distributions of evolving numerical tangential wind fields to those reproduced by the WW model. The fitted model parameters take on more than one value at different heights, as shown in the right panels of the figure. Some of the parameters, particularly k and n , run roughly parallel to each other. It should be mentioned that the vertical profiles of λ remain unchanged above the normalized height of about 0.2. Since the Levenberg-Marquardt method is designed to solve unconstrained nonlinear least squares problems for curve-fitting applications, the method does not use the constraints. Without imposing a constraint on the λ parameter, the method causes the parameter to wander into physically unrealistic parts of the parameter space. A range of λ needs to be constrained within $0 < \lambda \leq 10$. Future work will concentrate on refining the fitting algorithm by incorporating strong constraints that prevent the model parameters from drifting into any part of the space. In spite of the unconstraints in the LM method, dual inspections and comparisons of the tangential wind distributions between the numerical and parametric models suggest that the parametric model agrees reasonably well with the numerical model. Furthermore, the parametric model does a good job of calculating an approximation of the numerical vortex wind fields.

It is possible to construct a vertical distribution of tangential wind structure (e.g., Fig. 3) if the parameters varying with heights are accurately determined. For example, the model parameters may be expressed analytically as a function of height such that $V_x = V_x(z)$, $R_x = R_x(z)$, $k = k(z)$, $n = n(z)$ and $\lambda = \lambda(z)$. Knowledge of the vertical structure of the vortex is of great importance to engineers who express their interest in building sturdy residential and commercial structures that can withstand the damaging winds in tornadoes.

5. CONCLUSIONS AND FUTURE PLAN

The Wood-White parametric model mainly designed to depict a realistic-looking tangential wind profile that could better fit a realistic vortex was presented. The WW profile employed five key parameters: maximum tangential wind, radius of maximum tangential wind, and three power-law exponents that shaped different portions of the velocity profile, including the region of the highest tangential wind that can be made either broad or sharply-peaked. The effectiveness and versatility of the parametric model were successfully tested and validated against

the theoretical vortex solution of the unsteady BR vortex model and one high-resolution numerical vortex model of Trapp (2000) that represented evolving simulated vortices. Radial profiles of the parametric and numerical tangential wind profiles at each height were constructed to display a two-dimensional tangential wind structure in the cylindrical (r, z) model domain. Detailed comparisons between the parametric and numerical tangential wind profiles suggest that the WW model performed very well with low values of root-mean-square errors and high values of correlation coefficients. Hence, the capability of the WW model to reproduce the complex tangential wind fields has been examined.

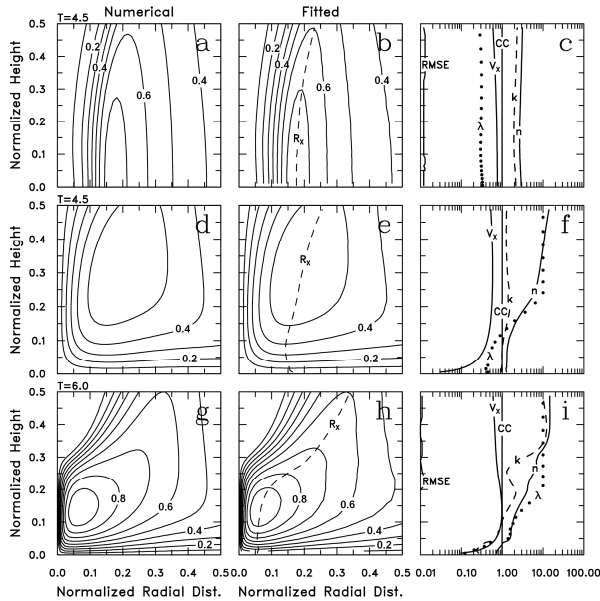


Fig. 3. Plots of numerical tangential velocity of Trapp (2000) for the free-slip experiment at (a) $t = 4.5$ min and the no-slip experiment at (d) $t = 4.5$ min and (g) $t = 6.0$ min. Plots of fitted tangential velocity of the WW model for the free-slip experiment at (b) $t = 4.5$ min and the no-slip experiment at (e) $t = 4.5$ min and (h) $t = 6.0$ min. All contours are normalized with interval of 0.1. Dimensionless radial distances and heights, respectively, are normalized by $r^* \equiv r/R$ and $z^* \equiv z/H$. Vertical profiles of the fitted parameters (V_x , k , n , λ), RMSE and CC are indicated in the panels (c), (f) and (i). Note that in these panels, the abscissa is logarithm to enhance readability. Dashed curves represent the vertical profiles of the fitted R_x in panels (b), (e) and (h).

The WW parametric model offers a few potential applications. One of them is analytical or model initialization that can be defined an initial condition of realistic-looking tangential velocity component varying radial distance and/or axial distance. Dowell et al. (2005), for example, used the Rankine model and the

Fiedler (1989, 1994) tangential-wind profile to imitate the Fiedler and Rankine vortices in their high-resolution numerical models. They studied how one- and two-dimensional distributions of particles motions and concentrations responded to evolving tornado-like vortex flows.

In the near future, application of the WW parametric model to any mobile or ground-based Doppler radar measurements including the dataset collected during the Second Verification of the Origins of Rotation in Tornadoes Experiment (VORTEX2) field program is planned.

6. ACKNOWLEDGMENTS

The authors would like to thank Rodger Brown for helpful comments and discussions that led to the improvement of this paper. Also, the authors are very grateful to Jeff Trapp of Purdue University for kindly supplying his numerical model data.

7. REFERENCES

- Burgers, J. M., 1948: A mathematical model illustrating the theory of turbulence. *Adv. Appl. Mech.*, **1**, 197-199.
- Davies-Jones, R. P., and V. T. Wood, 2006: Simulated Doppler velocity signatures of evolving tornado-like vortices. *J. Atmos. Oceanic Technol.*, **23**, 1029-1048.
- Dowell, D. C., C. R. Alexander, J. M. Wurman, and L. J. Wicker, 2005: Centrifuging of hydrometeors and debris in tornadoes: Radar-reflectivity patterns and wind-measurement errors. *Mon. Wea. Rev.*, **133**, 1501-1524.
- Fiedler, B. H., 1989: Conditions for laminar flow in geophysical vortices. *J. Atmos. Sci.*, **46**, 252-259.
- _____, 1994: The thermodynamic speed limit and its violation in axisymmetric numerical simulations of tornado-like vortices. *Atmosphere-Ocean*, **32**, 335-359.
- Holland, A. P., A. J. Riordan, and E. C. Franklin, 2006: A simple model for simulating tornado damage in forests. *J. Appl. Meteor. Climatol.*, **45**, 1597-1611.
- Holland, G. J., 1980: An analysis model of the wind and pressure profiles in hurricanes. *Mon. Wea. Rev.*, **108**, 1212-1218.
- _____, J. I. Belanger, and A. Fritz, 2010: A revised model for radial profiles of hurricane winds. *Mon. Wea. Rev.* (In press.)
- Jakobsen, F. and H. Madsen, 2004: Comparison and further development of parametric tropical cyclone models for storm surge modeling. *J. Wind Eng. Ind. Aerodyn.*, **92**, 375-391.
- Levenberg, K., 1944: A method for the solution of certain problems in least squares. *Quart. Appl. Math.*, **2**, 164-168.
- MacAfee, A. W., and G. M. Pearson, 2006: Development and testing of tropical cyclone parametric wind models tailored for midlatitude application – Preliminary results. *J. Appl. Meteor. Climatol.*, **45**, 1244-1260.

- Marquardt, D., 1963: An algorithm for least squares estimation on nonlinear parameters. *SIAM J. Appl. Math.*, **11**, 431-441.
- Phadke, A. C., C. D. Martino, K. F. Cheung, and S. H. Houston, 2003: Modeling of tropical cyclone winds and waves for emergency management. *Ocean Engineering*, **30**, 553-578.
- Press, W. H., S. A. Teukolsky, W. T. Vetterling, and B. P. Flannery, 1992: *Numerical Recipes in Fortran 77: The Art of Scientific Computing*. 2nd ed., Cambridge University Press, 933 pp.
- Rankine, W. J. M., 1882: *A Manual of Applied Physics*. 10th ed., Charles Griff and Company, London, 663 pp.
- Rott, N., 1958: On the viscous core of a line vortex. *Z. Angew. Math. Physik*, **9**, 543-553.
- Trapp, R. J., 2000: A clarification of vortex breakdown and tornadogenesis. *J. Atmos. Sci.*, **128**, 888-895.
- Willoughby, H. E., and M. E. Rahn, 2004: Parametric representation of the primary hurricane vortex. Part I: Observations and evaluation of the Holland (1980) model. *Mon. Wea. Rev.*, **132**, 3033-3048.
- _____, R. W. R. Darling, and M. E. Rahn, 2006: Parametric representation of the primary hurricane vortex. Part II: A new family of sectionally continuous profiles. *Mon. Wea. Rev.*, **134**, 1102-1120.
- Wood, V. T., and L. W. White, 2011: A new parametric model of vortex tangential-wind profiles: Development, testing and verification. *J. Atmos. Sci.*, (Submitted).
- Wurman, J., C. Alexander, P. Robinson, and Y. Richardson, 2007: Low-level winds in tornadoes and potential catastrophic tornado impacts in urban areas. *Bull. Amer. Soc.*, **88**, 31-46.